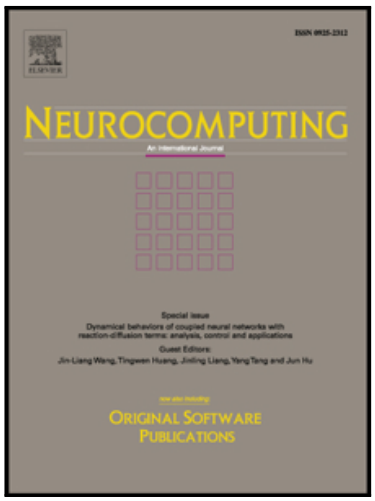

Spiking Pattern Recognition Using Informative Signal of Image and Unsupervised Biologically Plausible Learning

Soheila Nazari , Karim faez

PII: S0925-2312(18)31299-2
DOI: https://doi.org/10.1016/j.neucom.2018.10.066
Reference: NEUCOM 20123

To appear in: *Neurocomputing*

Received date: 6 November 2017
Revised date: 17 September 2018
Accepted date: 30 October 2018

Please cite this article as: Soheila Nazari , Karim faez , Spiking Pattern Recognition Using Informative Signal of Image and Unsupervised Biologically Plausible Learning, *Neurocomputing* (2018), doi: https://doi.org/10.1016/j.neucom.2018.10.066

Spiking Pattern Recognition Using Informative Signal of Image and Unsupervised Biologically Plausible Learning

Soheila Nazari, Karim faez*

Department of Electrical Engineering, Amirkabir University of Technology, Tehran, Iran
*Corresponding author. Tel: +989190721964, Email address: kfaez@aut.ac.ir

Abstract

The recent progress of low-power neuromorphic hardware provides exceptional conditions for applications where their focus is more on saving power. However, the design of spiking neural networks (SNN) to recognize real-world patterns on such hardware remains a major challenge ahead of the researchers. In this paper, SNN inspired by the model of local cortical population as a biological neuro-computing resource for digit recognition was presented. SNN was equipped with spike-based unsupervised weight optimization based on the dynamical behavior of the excitatory (AMPA) and inhibitory (GABA) synapses using Spike Timing Dependent Plasticity (STDP). This biologically plausible learning enables neurons to make decisions and learns the structure of the input examples. There are two main reasons why this structure is state of the art compared to previous works: learning process is compatible with many experimental observations on induction of long-term potentiation and long-term depression, image to signal mapping created an informative signal of the image based on sequences of prolate spheroidal wave functions (PSWFs). The proposed image mapping translates the pixels attributes to the frequency, phase, and amplitude of a sinusoidal signal. This mapping enables the SNN to generalize better to the realistic sized images and significantly decreases the size of the input layer. Cortical SNN compared to earlier related studies recognized MNIST digits more accurate and achieved 96.1% classification accuracy with unsupervised learning based on sparse spike activity.

Keywords
Spiking Neural Network, STDP, AMPA and GABA current, Digit Recognition, Image coding.

1- Introduction

The power consumption that the mammalian neo-cortex consumes in cognitive and pattern recognition functions is between 10 and 20 watts [1]. There is strong incentive to reduce power consumption of chips because energy consumption is a fundamental factor in the performance of a system [2]. Hardware implementations of spiking neural network that has been done in recent years on the neuromorphic chip [3-6], as a power-efficient system, for transmitting each spike only consume a few nJ or even pJ [7-9]. In some recent cases, consumption is less than 0.02 pJ per spike [10] and consequently only a few pW per synapse [11], so that, the proper performance of neuromorphic systems makes them possible to implement on-chip learning mechanisms on these hardware [4,12-13].

Until now, achieving good performance in identifying patterns such as MNIST dataset [14] using the spiking network remains a challenge. There are two main approaches to designing and training spiking networks for machine learning applications such as pattern recognition that these concepts of neural theories have categorized as spike-based [15-19] and rate based learning. There is considerable debate on the importance of firing rate or timing of spikes. Scientists agree on the importance of both rate and spike timing in the brain coding. The basis of learning based on the spike is the change in the weight of network synapses using different views of the spike-timing-dependent plasticity (STDP). While, the training rule in rate-based learning define based on back-propagation [20] or other rate-based learning algorithms [8, 21-23]. Considering the efficient power consumption have a significant effect on the technology of neuromorphic hardware, on the other hand, the learning process itself requires high power consumption, therefore, more attention is being paid to spike-based learning versus rate-based learning [24].

This article is the first step aimed at developing a technical training for the spiking network based on empirical observations of the process of brain learning. Here a biologically plausible computational SNN was presented that was trained based on the spike-based learning by updating the values of the GABA and AMPA synaptic strength in an unsupervised fashion using STDP, in other words, the synaptic weights of the network learn the structure of the input pattern without using the label.

Unlike most previous works, the number of neurons in the input layer was not proportional to the image pixels [23-26]. Using the information encoding of the image pixels into the frequency, phase, and amplitude of the sine signal, one neuron forms the input layer of pattern recognition network. This conversion makes proposed network as a general platform for pattern recognition, which is independent of image pixels. This new concept speeds up the computation of the input layer and gives the possibility to the network to be applicable for realistic sized images. Except image to signal mapping, no other pre-processing performed on the data. We achieved a performance of 96.1% using 5010 learning neurons with the adopted structural of the local cortical population.

In the next section, the method including the neuron and synapse model, network architecture, training and learning process have explained. Section III contains the simulation results and comparison to those of other previous architectures and finally, section IV concludes the paper.

2- Methods

Over the past few decades, biologically inspired computing (adopted computational models of the brain structure) have introduced as the most powerful tools for the pattern recognition, development of novel problem-solving techniques and classification problem [1]. Such studies tried to develop the structural and functional models of neuron and synapse based on the biological reality of the nervous system to provide an efficient pattern recognition tool in the cognitive applications. To achieve this goal, a local cortical population with the bio-inspired computational model of excitatory (inhibitory) AMPA-type (GABA-type) synaptic current and neurons was presented as the spiking platform of digit recognition. The structure of SNN was configured with c++ language on the Visual Studio software.

In this section, the dynamics of neurons, AMPA and GABA current, the pattern recognition architecture contains image coding and network layers have described. Then learning mechanism based on biological evidence has explored and eventually, the MNIST training and classification procedure has explained.

2.1- Neuron and Synapse Model

Dynamic of neurons are described by leaky integrate and fire model. Membrane potential $v_k(t)$ of neuron *k* defined by the following equation [27]:

$$\tau_m \frac{dv_k}{dt} = -v_k(t) + I_{AK}(t) - I_{GK}(t) \quad (1)$$

Membrane time constant $\tau_m$is 20 ms for excitatory neurons and 10 ms for inhibitory neurons [28]. The received excitatory and inhibitory synaptic current by neuron k, denoted with I_{Ak} (AMPA current) and I_{Gk} (GABA current), respectively. Resting potential (v_{res}) of all neurons is equal to zero. The threshold of neurons firing (v_{thr}) has considered 18 mv above resting potential. With more complementary expression, when the membrane potential passes the threshold value, the neuron potential falls to resting potential and the neuron can't fire again for a refractory time τ_{rp} which is 2 ms for excitatory neurons and 1 ms for inhibitory neurons. Excitatory and inhibitory synaptic currents of neuron k can be obtained using auxiliary variables x_{Ak}, x_{Gk} as follow:

$$\tau_{dA} \frac{dI_{Ak}}{dt} = -I_{Ak} + x_{Ak} \quad (2)$$

$$\tau_{rA} \frac{dx_{AK}}{dt} = -x_{Ak} + \tau_m \left(J_{k-Pyr} \sum_{pyr} \delta(t - t_{k-pyr} - \tau_L) + J_{k-ext} \sum_{ext} \delta(t - t_{k-ext} - \tau_L) \right) \quad (3)$$

$$\tau_{dG}\frac{dI_{Gk}}{dt} = -I_{Gk} + x_{Gk} \quad (4)$$

$$\tau_{rG}\frac{dx_{Gk}}{dt} = -x_{AG} + \tau_m(J_{k-int}\sum_{int}\delta(t - t_{k-int} - \tau_L)) \quad (5)$$

Where $t_{k-pyr,int,ext}$ is the spike time received from pyramidal neurons/interneurons/external inputs connected to neuron k. Decay and rise time of the AMPA-type (GABA-type) synaptic current denoted by $\tau_{dA}(\tau_{dG})$ and $\tau_{rA}(\tau_{rG})$, respectively. The latency of the post-synaptic currents is $\tau_L = 1$ ms. The efficacy of the connections from pyramidal neurons/interneurons/external inputs on neurons k defined with $J_{k-pyr,int,ext}$ which has a fundamental role in the learning procedure. In Eq.3, the sum of the Dirac function ($\sum_{pyr}\delta(t - t_{k-pyr} - \tau_L)$) indicates the spikes that are received by neuron *k* from pyramidal neurons. Because all pyramidal neurons connected to neuron k with the fix weight J_{k-Pyr}, the sum of the Dirac function multiplied by J_{k-Pyr} which denotes the received excitation from pyramidal neurons to neuron *k.*

2.2- Network Architecture

The proposed pattern recognition structure consists of three parts: the input layer, the population of 5,000 neurons and 5 million excitatory and inhibitory synapses as a second layer and output layer.

2.2.1- Input layer

MNIST dataset as the input of network contains 60,000 training examples and 10,000 test examples of 28*28 pixel images of the digits 0 to 9 [14]. Previous studies [23-26] considered one-to-one correspondence between the input image pixels and the input layer neurons. Unlike this method, we offered the image to signal mapping to convert the image to the one-dimensional sinusoidal signal to make the input layer of the spiking network independent of the image pixels. With this conversion, the image has injected into the second layer through one input neuron. Therefore, despite image information retention, the size of input layer significantly reduced.

Meijer in 1992 [29] translated the image into an auditory signal. His conversion procedure translated the vertical and horizontal position of the pixel into the frequency and time-after-click. This mapping proposed for auditory system application. Here, the image was translated into the informative signal. The proposed conversion procedure translates the vertical and horizontal position of the pixel into the frequency and phase of the sine signal with the amplitude proportional to the pixel brightness. To clarify this mapping, according to Fig.1, it is obvious that prolate spheroidal wave sequence consists of sine signals with different amplitude, frequency, and phase [30]. Encoding the main information of the image pixels into the frequency, phase, and amplitude of the sine signals gives us a series of sine signals with a different amplitude, phase, and frequency similar to the sequence of prolate spheroidal wave functions

(PSWFs). In fact, the image has transformed into a set of sequences of the PSWF as an informative signal.

We proved that the second layer of the present pattern recognition network as an information channel transmits the information of the input pattern in the form of PSWF coefficients to the power spectrum of the output local field potential (LFP) [31]. Since the second layer of pattern recognition network decodes the information in the form of PSWF coefficients, encoding image information into the prolate spheroidal wave sequence and the brain-compatible learning approach (discussed in section 2.3), enable the proposed spiking platform to recognize digits more accurate than previous approaches.

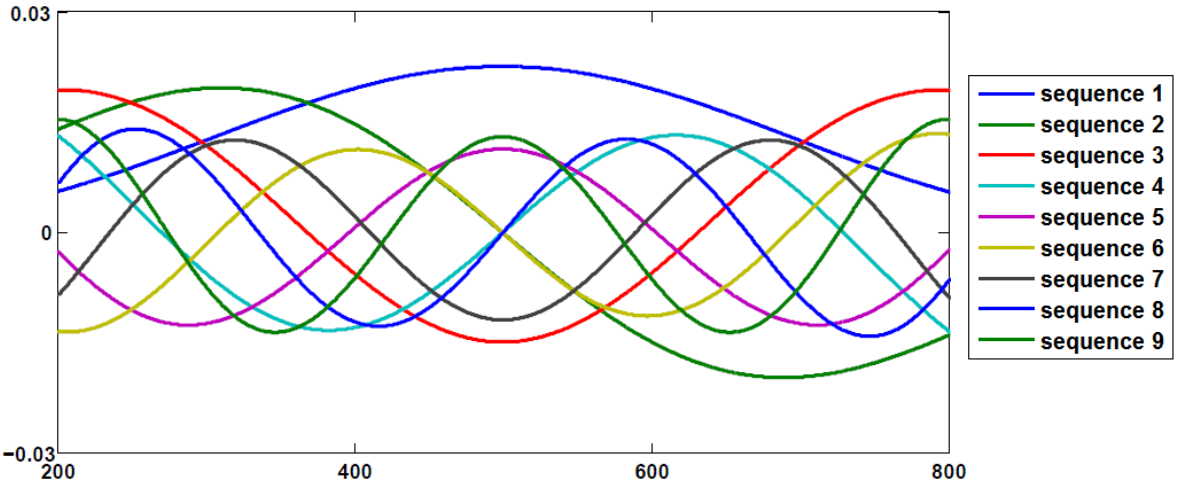

Fig.1: Consecutive sequences of prolate spheroidal wave functions, which were used for image coding.

To calculate informative signal of image, the image has been considered as an M(rows)*N(columns) pixel matrix as follows:

$image = P_{i,j} \qquad i = 1, \dots, M \;\; \& \;\; j = 1, \dots, N$

In the process of conversion, horizontal position, vertical position, and brightness of each pixel was translated into the frequency, phase, and amplitude of the sine signal, respectively which is shown in Fig.2. Given that the frequency variation range is less than the phase, in the dataset that has fewer rows than the number of columns, we must switch translation order.

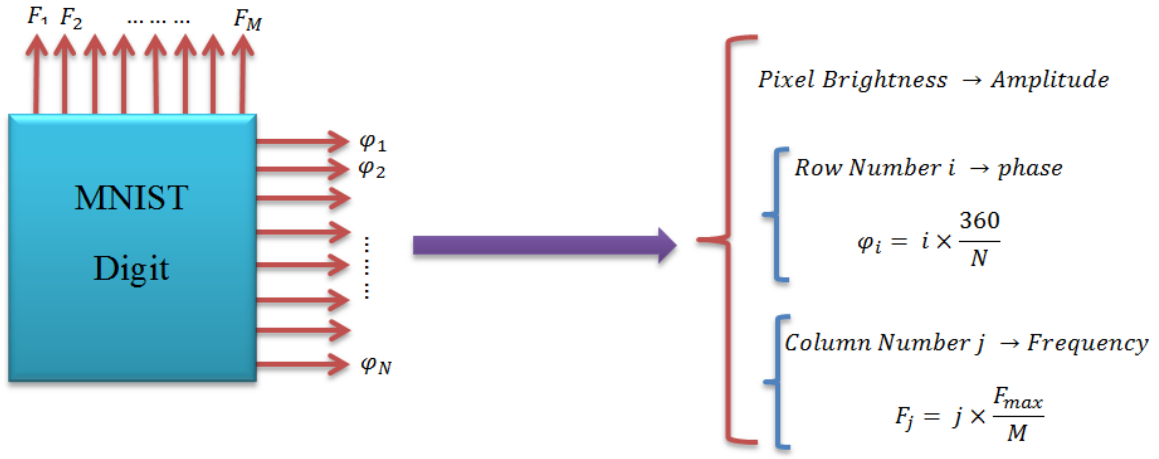

Fig.2: Information of image was encoded in the frequency, phase, and amplitude of the sinusoidal signal (F_{max} = 150 Hz).

Fig.3 indicates the principles of the proposed approach in the mapping of the image to the informative signal. Proportional to the informative signal of the MNIST patterns, the time-varying rate of Poissonian spike trains was presented to the second layer.

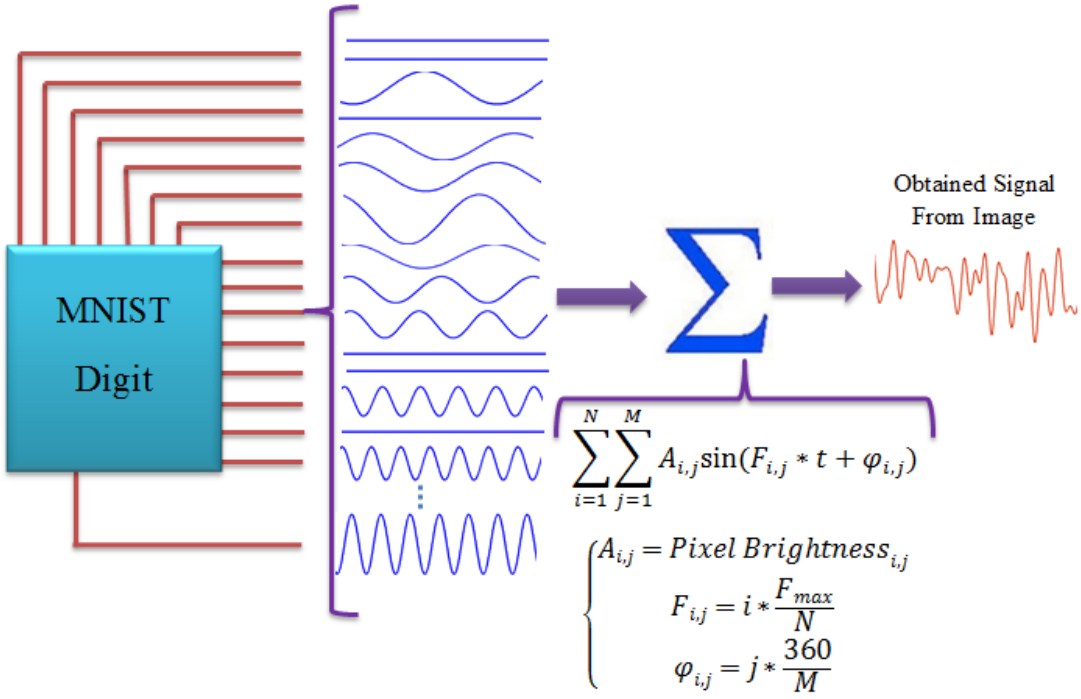

(a)

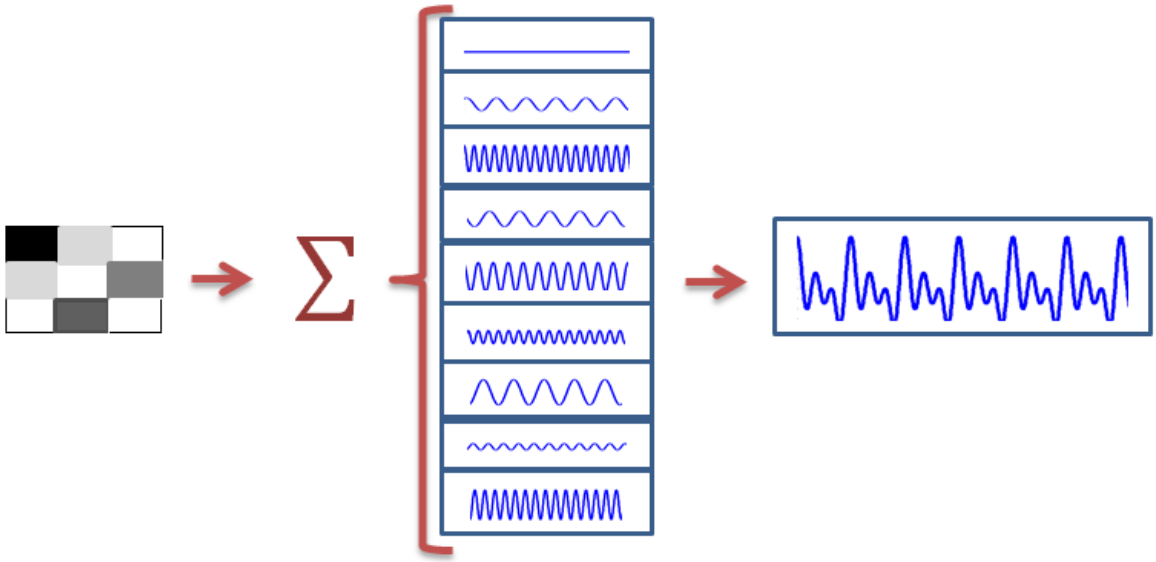

(b)

Fig.3: (a) Proposed mapping translated the information of the image into the sine signal to decrease the input size of the network significantly. This makes the network size more reasonable in the realistic sized images. (b) The example of the informative signal of the image based on the sequence of prolate spheroidal wave functions.

Therefore, each pixel of the image corresponds to a sinusoidal wave with a specific amplitude, frequency, and phase, derived from the proposed coding approach of Fig.2. The informative signal of the image was calculated by the sum of the sine signals of each pixel. If any of the image pixels are displaced, the informative signal of the image will also be different. This not only does not limit the network performance but also improves the recognition accuracy of the network. In fact, different patterns have a unique informative signal and the informative signal of the patterns that are classified in one category contain a high percentage of matching between their PSWF coefficients.

2.2.2- Second layer

The spiking network based on biological evidence as a second layer is composed of N= 5000 neurons. Based on experimental observations, 80% of the neurons are excitatory (Pyramidal Neurons (PY)) and 20% are inhibitory (Interneurons (IN)) [32]. Both pyramidal neurons and interneurons described by the dynamics of the leaky integrate and fire (LIF) neurons [33]. Presynaptic neurons excite or inhibit

postsynaptic neurons. To clear the neuronal interaction in the second layer, the structural connectivity of the limited neurons (two interneurons and two pyramidal neurons) has shown in Fig.4.

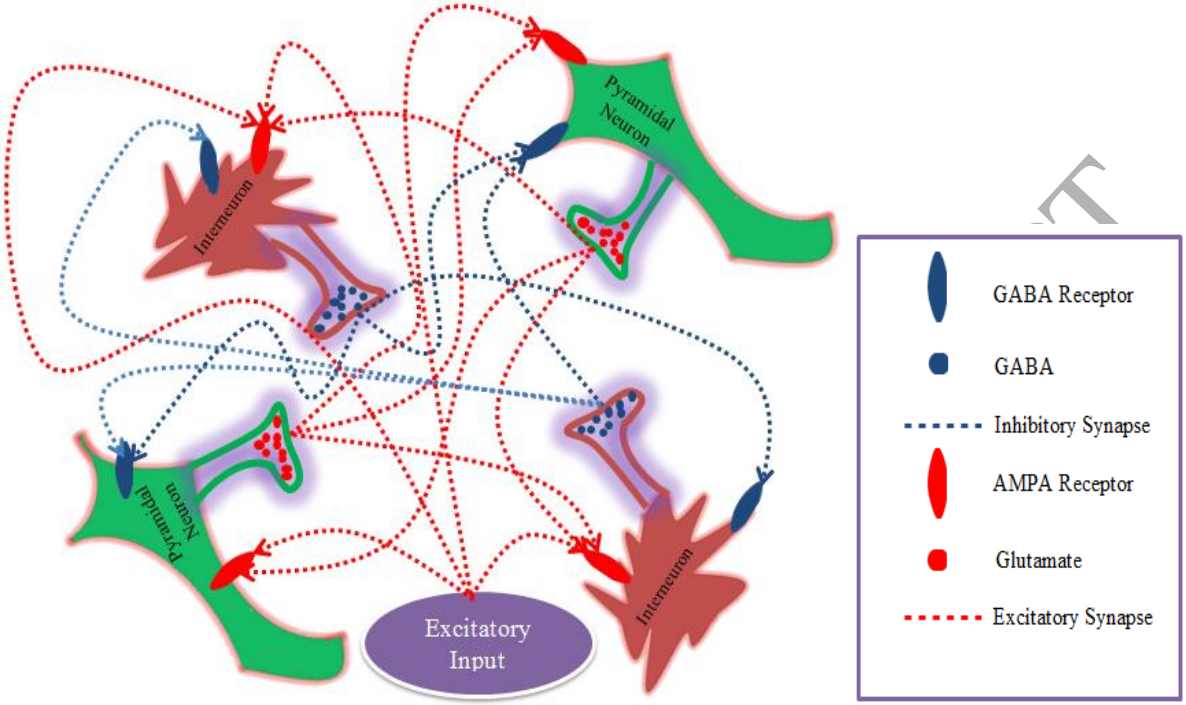

Fig.4: A partial view of the excitatory and inhibitory interaction of pyramidal neurons and interneurons on each other has been shown. Through the synaptic connections and AMPA and GABA receptors, neurons have excitatory and inhibitory effects on their connected neurons.

The paper emphasizes that the spiking network have modeled based on the dynamical quiddity of the nervous system and the brain-compatible learning approach was used to train it. Therefore, the spiking network has been used which produces spike-activity in accordance with the recorded data of thalamus of an anesthetized monkey [27]. Thus the computational model of the pyramidal neuron, interneuron, excitatory and inhibitory synapses AMPA and GABA and also the ratio of pyramidal neurons to interneurons and connection probability between any directed pair of cells was adapted from [27]. On the other hand, the configuration of the spiking pattern recognition network on the neuromorphic hardware has attracted a lot of attention [34-36]. Fully connected neural networks have shown excellent performance on a wide range of recognition and classification tasks. However, their hardware implementations currently suffer from large silicon area and high power consumption due to their high degree of complexity. On the other hand, some studies proved that the number of connections in fully connected networks can be decreased by up to 90% while improving the performance accuracy on three popular datasets (MNIST, CIFAR10, and SVHN) which emphasize on the advantages of the sparsely-

connected networks [37]. Therefore, all neurons in the second layer are connected randomly, which the connection probability between any directed pair of neurons is 0.2 [38-39]. This means that each neuron of second layer is connected to approximately 1000 neurons of the second layer. Therefore, over 5 million (exactly 5001605) excitatory and inhibitory synapses have formed in the spiking network of second layer. The connections map of the second layer neurons has shown in Fig.5.

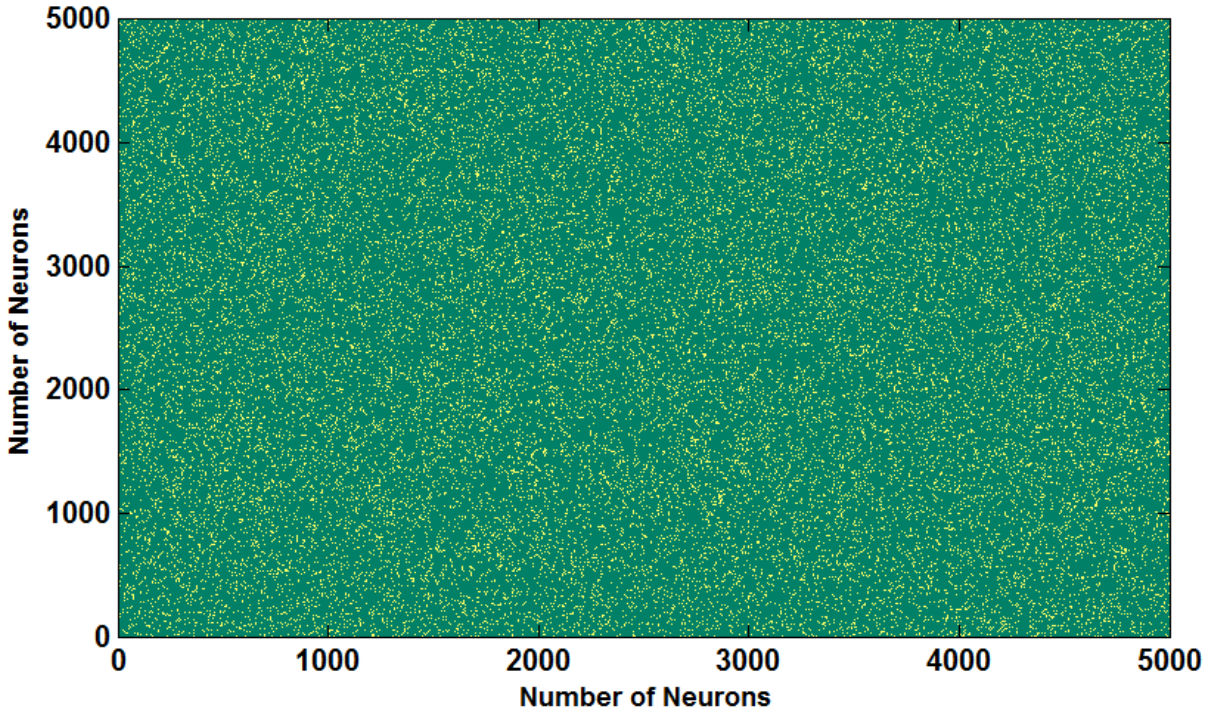

Fig.5: The connections pattern of 4000 pyramidal neurons and 1000 interneurons. Each point indicates the connection between the two corresponding neurons so that over 5 million synapses have considered in the neuronal population.

The informative signal of image injected to the second layer for 600 ms in the form of Poisson-distributed spike trains. The time-varying rate of Poissonian spike trains (an example of test-set of digit 2) has shown in Fig.6.

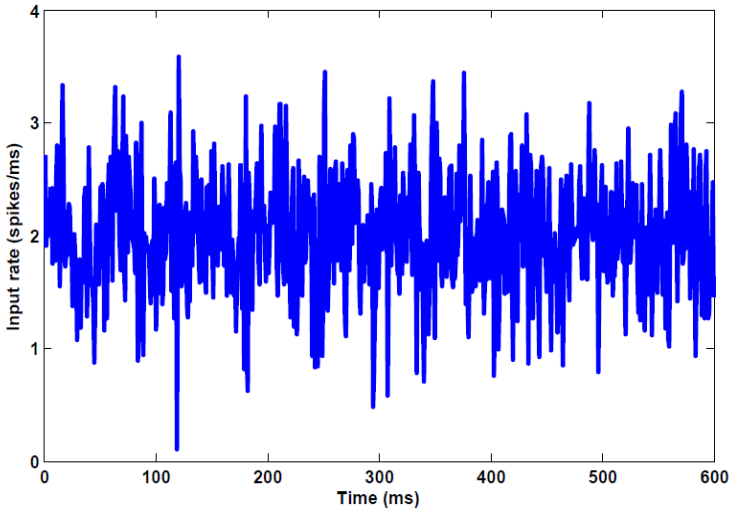

Fig.6: The time-varying rate of Poissonian spike trains was delivered to the second layer neurons in a 600 ms long interval.

In fact, the time-varying rate of Poisson spike trains with the mean of informative signal of image was injected to the second layer. Each neuron is receiving an external excitatory synaptic input. These synapses are activated by the Poisson spike trains with a time varying rate, which is identical for all neurons. Therefore, time varying rate of excitatory input is equal to informative signal of image. The structure of the pattern recognition network, the training method, and the converter, which transforms informative signal of image to spike train are based on biological evidence [27].

2.2.3- Output layer

The output layer of the pattern recognition network consists of 10 LIF neurons with the full connection to the second layer neurons by the excitatory and inhibitory synapses. Neurons in this layer (classifying neurons) are responsible for classification of digits. The general structure of the considered architecture in digit recognition has presented in Fig.7.

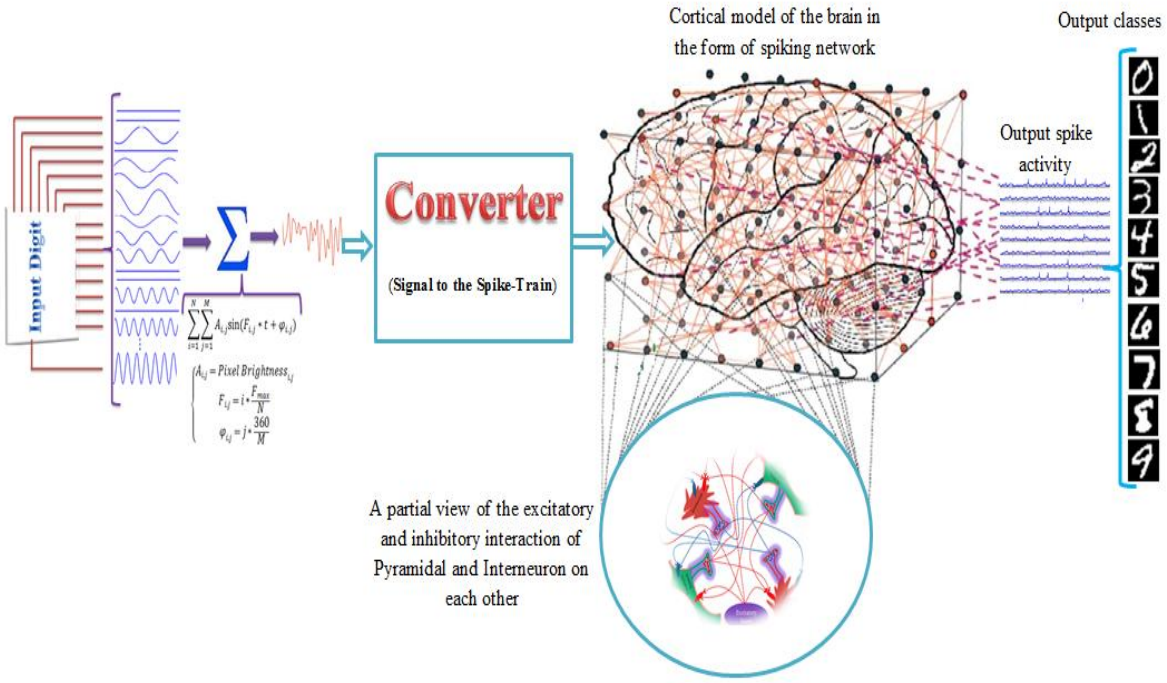

Fig.7: The general scheme of the proposed configuration for pattern recognition based on the bio-inspired spiking network.

Different spiking neurons have been proposed which contain various computational cost and complexity of spiking behavior. Type of the problem determines the model of the spiking neuron. Models of biological richness such as Hodgkin-Huxley neuron model are suitable when the goal is to study how the neuronal behavior depends on measurable physiological parameters. Of course, in this case, only a limited number of the coupled spiking neurons can be simulated in real time. In contrast, the most efficient spiking neuron model in the real-time simulation of thousands of neurons is LIF model [40]. In this paper, it is true that a simple neuron model has been used, but the dynamical model of AMPA-type and GABA-type current create complex dynamical interaction, which forms uniquely pattern recognition platform.

The method of training of classifying neurons is similar to the neurons of the second layer. Classifying neurons trained with spike-based unsupervised weight optimization based on the dynamical behavior of the excitatory (AMPA) and inhibitory (GABA) synapses using Spike Timing Dependent Plasticity (discussed in section 2.3).

2.3- Learning

Computers in cognitive issue are not at the level of competition with the human brain. To reach this valuable goal, changing the basis of computation to the spike-base computation and using the concepts of biological systems in solving computer science problems such as advanced search and optimization algorithms can play a decisive role. This new field ultimately leads to design bio-inspired software or in-silico chips based on the behavior of structural components of the brain [41-43]. Researchers' efforts in recent decades have caused that spiking networks have appeared as the effective and efficient architectures to imitate brain function. Information coding in the spiking networks are temporally and the neurons communication create through spike transmission via synapses. In such networks, the function of the spike-timing-dependent-plasticity mechanism depends on the temporary information of the released spikes from other neurons, which make it possible to schedule the online weight allocation of synapses. This paper, as a first step, has worked on promoting the STDP learning process from the perspective of importing the biological concept of AMPA and GABA current in synaptic space into the dynamical model of spiking network. STDP is a biological approach similar to the Hebbian learning [44-45] that adjusts the strength of connections between neurons in the brain. In other words, STDP modifies the synaptic weight between neurons based on the spiking activity of the pre and postsynaptic neurons and this process continues until these synaptic weight store characteristics information of pattern, which is necessary to transform a particular input pattern to its corresponding output.

Changes in synaptic strength between pre-synaptic neuron *i* and a post-synaptic neuron *j* based on the STDP rule has been characterizing as:

$$\Delta w_j = \sum_{k=1}^{N} \sum_{l=1}^{N} W(t_j^l - t_i^k) \tag{6}$$

Here, the constant N is equal to 5010. It shows the number of neurons in the pattern recognition network (5000 neurons of second layer and 10 neurons of output layer) which participate in the training procedure. Based on spike time of pre and post-synaptic neurons, increases or decreases in synaptic strength with the function W(x) expressed as [46]:

$$W(x) = \begin{cases} A_+ \exp\left(\frac{-x}{\tau_+}\right) & if\ x > 0 \\ A_- \exp\left(\frac{x}{\tau_-}\right) & otherwise \end{cases} \tag{7}$$

In Eqs.6,7, t_j^l defines the l^{th} spike time of neuron *j*; similarly, t_i^k represents the k^{th} spike time of neuron *i*; constant parameters A_+ and A_- are representative of the amplitude of weight changing (at $t = 0_+$ and $t = 0_-$, respectively) and exponential decrease in function W(x) expresses with the time constants τ_+ and τ_-. Fig.8 shows the change of the synaptic weights versus a function of the relative timing of pre- and postsynaptic action potentials. According Fig.8, two modes are possible: the weight of a synapse increased if a spike arrives prior to the firing of a neuron (long-term potentiation (LTP)), and decreased if

the spike arrives after the firing of a neuron (long-term depression (LTD)). In summary, the spike transmission from the post-synaptic terminal is an important factor in synaptic plasticity [46].

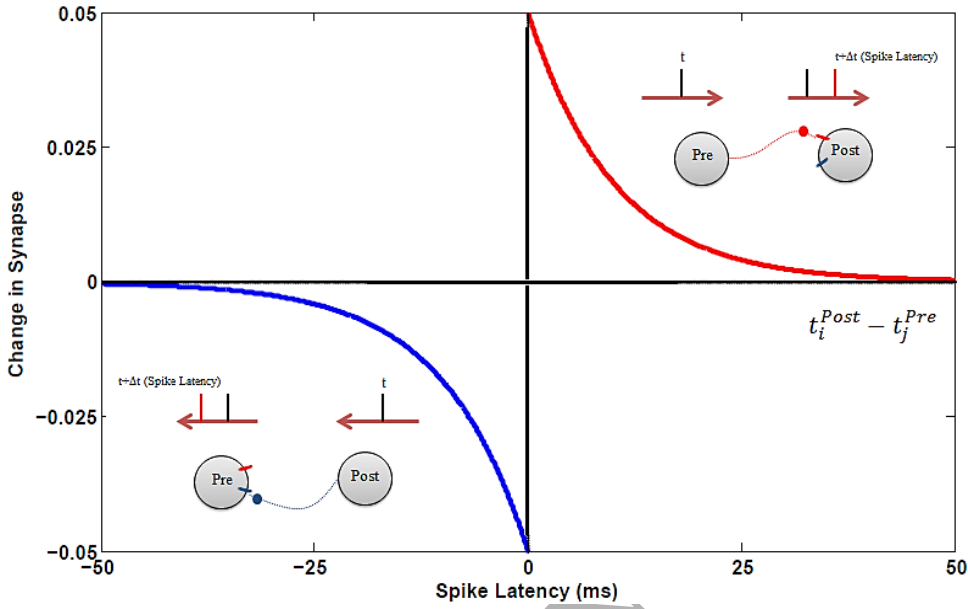

Fig.8: Model of STDP learning rule which contain LTP (post-synaptic neuron spike after pre-synaptic neuron $t_i^{post} - t_j^{pre} > 0$), and LTD (post-synaptic neuron spike before pre-synaptic neuron $t_i^{post} - t_j^{pre} < 0$).

The abundance of the number and type of biological cells, as well as unique paths that handle the accurate processing and transmitting of information in the brain, have made the understanding cellular processes and dynamical principles governing neural function very complicated. Tracking on the functional and structural performance of the variety of proteins such as ion channels, cell adhesion molecules, neurotransmitters, and anchoring can be useful to clarify the syntactic function and plasticity mechanism. Adjustment of neurotransmitters transmissions such as AMPA and GABA (the main excitatory and inhibitory neurotransmitters in the brain) is a fundamental mechanism for the synaptic transmission modulation and ultimately synapse plasticity, which is the basis of the proposed learning. Plastic changes of AMPA current rate in the synaptic space has been proved to play a crucial role in the information storing in the nervous system [47]. In other words, the regulated augmentation and diminution of the excitatory synaptic AMAP current in synaptic transmissions lead to the occurrence of LTP and LTD [48]. On the other hand, Long and short-term plasticity of cortical, incremental and decreasing synaptic connections are affected by inhibitory synaptic current GABA [49-50].

Based on these neuro-scientific evidences, the occurrence of biological phenomena LTP and LTD are affected by AMPA-type and GABA-type synaptic currents. In fact, The proposed learning idea is the combination of the two existing concepts: STDP learning approach and the effect of AMPA and GABA

synaptic current in learning. Some new topics in science came from the combination of existing concepts and became a new approach. Modeling approach provides the opportunity to explore new theory in the real world. The computational model of neurons, AMPA and GABA synapses was used to find out the new learning approach that has significant application in machine learning and artificial intelligence.

Therefore, the attempt was made to consider these scientific findings based on the corner of the biological reality of the brain mechanism in learning as the training mechanism of the proposed pattern recognition network. General equations for AMPA and GABA current in pyramidal neurons proposed as follow: ($A_+ > 0$ & $A_- < 0$)

$$\tau_{rA}\frac{dx_{AK}}{dt} = -x_{Ak} + \tau_m\left(\left[\sum_{pyr}\left(J_{k-Pyr} + (A\exp(-\frac{(t_k - t_{pyr})}{\tau_+}))\right)\delta(t - t_{k-pyr} - \tau_L)\right] + [J_{k-ext}\sum_{ext}\delta(t - t_{k-ext} - \tau_L)]\right) \quad A = \begin{cases} A_+ & if \quad t_k - t_{pyr} > 0 \\ A_- & if \quad t_k - t_{pyr} < 0 \end{cases} \tag{8}$$

$$\tau_{rG}\frac{dx_{AG}}{dt} = -x_{AG} + \tau_m\left(\sum_{int}\left(J_{k-int} + \left(\text{Aexp}\left(\frac{(t_k - t_{int})}{\tau_-}\right)\right)\right)\delta(t - t_{k-int} - \tau_L\right)$$

$$A = \begin{cases} A_- & if \quad t_k - t_{int} > 0 \\ A_+ & if \quad t_k - t_{int} < 0 \end{cases} \tag{9}$$

Eq.8 was developed as a training equation of excitatory synapses in pyramidal neurons. It is evident when the network is training, the connecting weights of all pyramidal neurons to the neuron k are not equal so that each pyramidal neuron attached to the neuron k with its own weight. Therefore, the efficacy of connections J_{k-Pyr} was multiplied by Dirac function and then summed.

Similarly, general equations for AMPA and GABA current in Interneurons proposed as follow: ($B_+ > 0$ & $B_- < 0, B = 0.4A$)

$$\tau_{rA}\frac{dx_{AK}}{dt} = -x_{Ak} + \tau_m\left(\left[\sum_{pyr}\left(J_{k-Pyr} + (B\exp(-\frac{(t_k - t_{pyr})}{\tau_+}))\right)\delta(t - t_{k-pyr} - \tau_L)\right] + [J_{k-ext}\sum_{ext}\delta(t - t_{k-ext} - \tau_L)]\right) \quad B = \begin{cases} B_+ & if \quad t_k - t_{pyr} > 0 \\ B_- & if \quad t_k - t_{pyr} < 0 \end{cases} \tag{10}$$

$$\tau_{rG}\frac{dx_{AG}}{dt} = -x_{AG} + \tau_m\left(\sum_{int}\left(J_{k-int} + \left(\text{Bexp}\left(\frac{(t_k - t_{int})}{\tau_-}\right)\right)\right)\delta(t - t_{k-int} - \tau_L\right)$$

$$B = \begin{cases} B_- & if \quad t_k - t_{int} > 0 \\ B_+ & if \quad t_k - t_{int} < 0 \end{cases} \tag{11}$$

2.4- Training and Classification

Pattern recognition network was trained on the training-set of MNIST (60,000 samples) ten times. Between two consecutive images, a time distance100 ms has considered to allow the network variables to reach their stable state. Network training has done unsupervised except the last step, which based on the highest firing activity to each class of digit, one output neuron was assigned to each input pattern. After the completion of training and in the testing step, network weights do not change and are considered constant. Therefore, after the training step, $\left(J_{k-Pyr} + (A\exp(-\frac{(t_k - t_{pyr})}{\tau_+}))\right)$, $\left(J_{k-int} + \left(\text{Aexp}\left(\frac{(t_k - t_{int})}{\tau_-}\right)\right)\right)$, $\left(J_{k-Pyr} + (B\exp(-\frac{(t_k - t_{pyr})}{\tau_+}))\right)$, $\left(\text{Bexp}\left(\frac{(t_k - t_{int})}{\tau_-}\right)\right)$ have been fixed. The highest rate of firing determines the winning classifying neuron in each test set. Therefore, the classification accuracy of the network on the MNIST test-set (10,000 samples) determines using the response of the class-assigned output neurons (classifying neurons).

3- Results

The proposed spike-based training method creates paths between the activated input pattern and the classifying neurons, which leads to the accurate categorization of the input patterns. In the test phase, all network parameters, including the weight of the synapses, are fixed. Fig.9 shows the performance of the network in recognizing digits with applying the MNIST training set in the first and tenth iteration of training. The number of spike activity in Fig.9 defines average firing rate of each classifying neuron in response to the activated input pattern through considering 60,000 samples of training MNIST dataset. As can be seen, in fig.9(a) as a first training iteration, the firing rate of the classifying neurons does not give us the correct result for the input pattern classification. Conversely, in the last training iteration (Fig.9(b)), the firing rate of classifying neurons classifies the training set of MNIST with the precision of 98.9%.

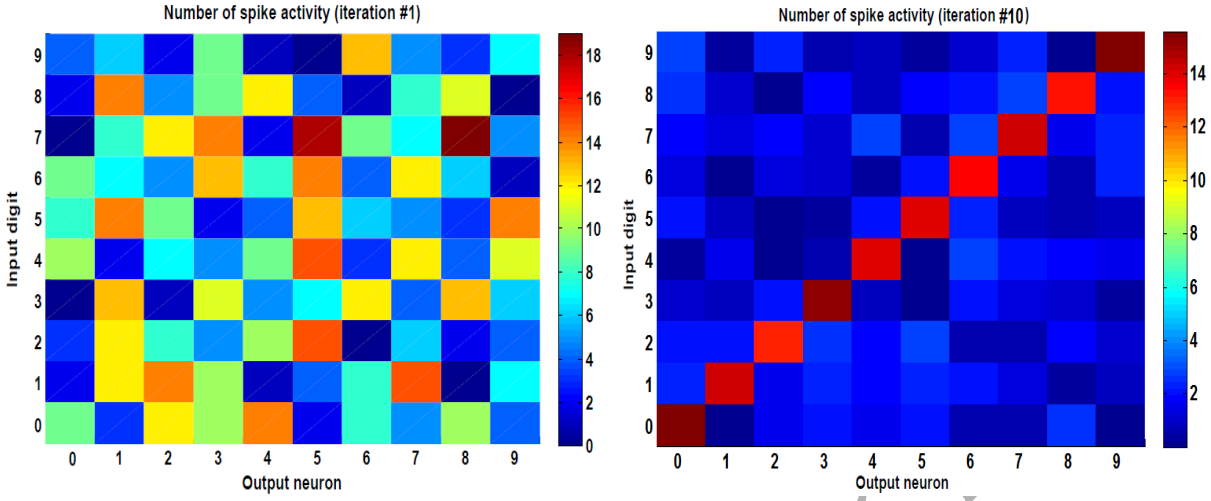

(a) (b)

Fig.9: (a),(b) indicate the average firing rate of each classifying neurons in response to the activated input pattern in the first and tenth training iteration, respectively. At the beginning of training, the firing rate of the classifying neurons is irregular and disturbed. Finally, at the end of the training, the classifying neurons have the most firing rate in response to their activated input patterns.

From another perspective, membrane potential and spike pattern of classifying neurons in response to the test patterns have shown in Fig.10. In Fig.10(a)-(e) digits 0,1,2,3,4 injected to the spiking pattern recognition network, respectively and the spike reaction of classifying neurons has shown in each part of Fig.10. As is evident, the firing rate of the classifying neurons in response to the test samples of MNIST categorized the input patterns well.

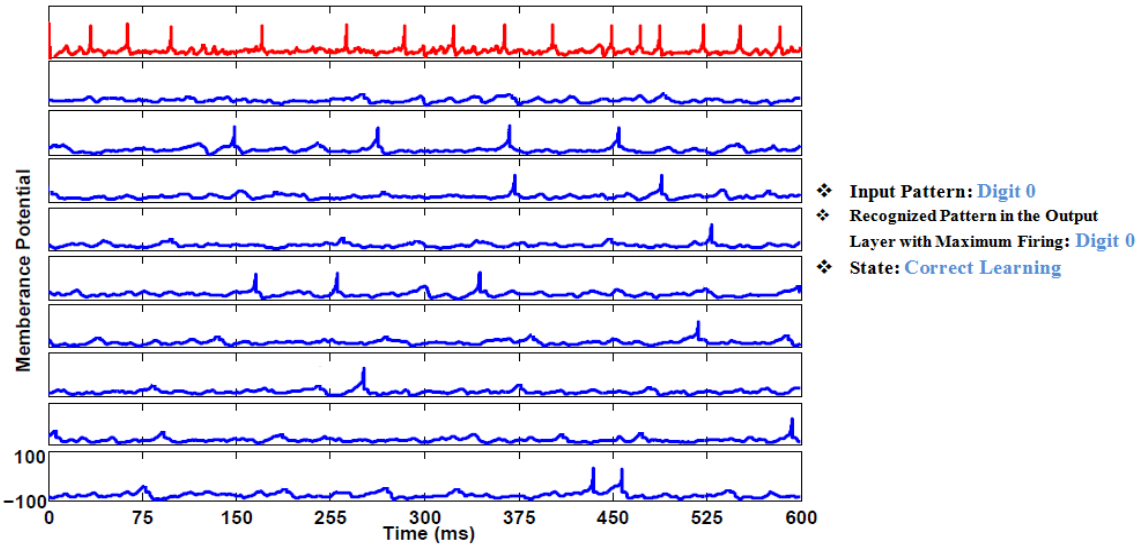

(a)

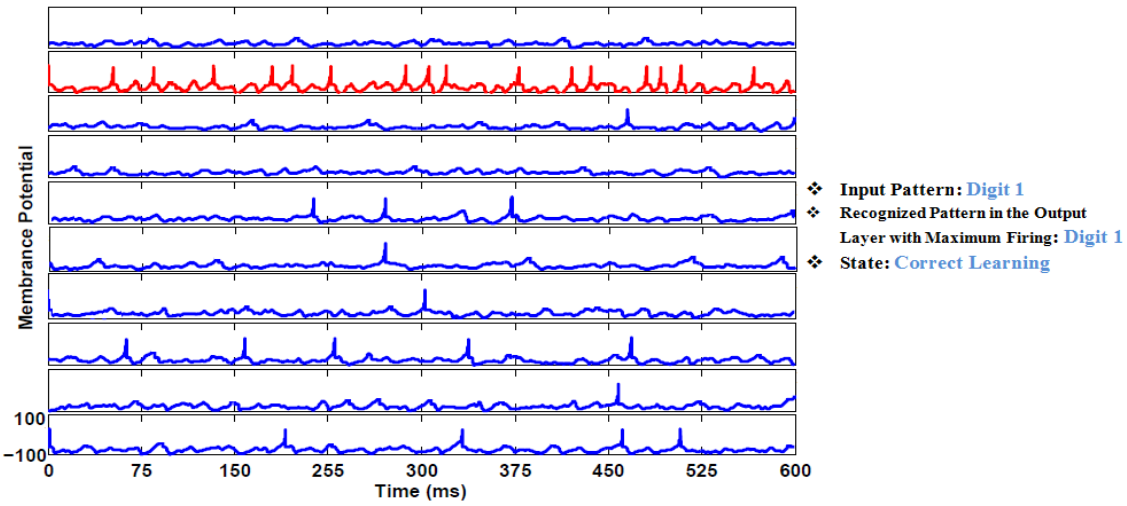
Membrance Potential
100
−100
0
75
150
255
300
375
450
525
600
Time (ms)
Input Pattern: Digit 1
Recognized Pattern in the Output Layer with Maximum Firing: Digit 1
State: Correct Learning

(b)

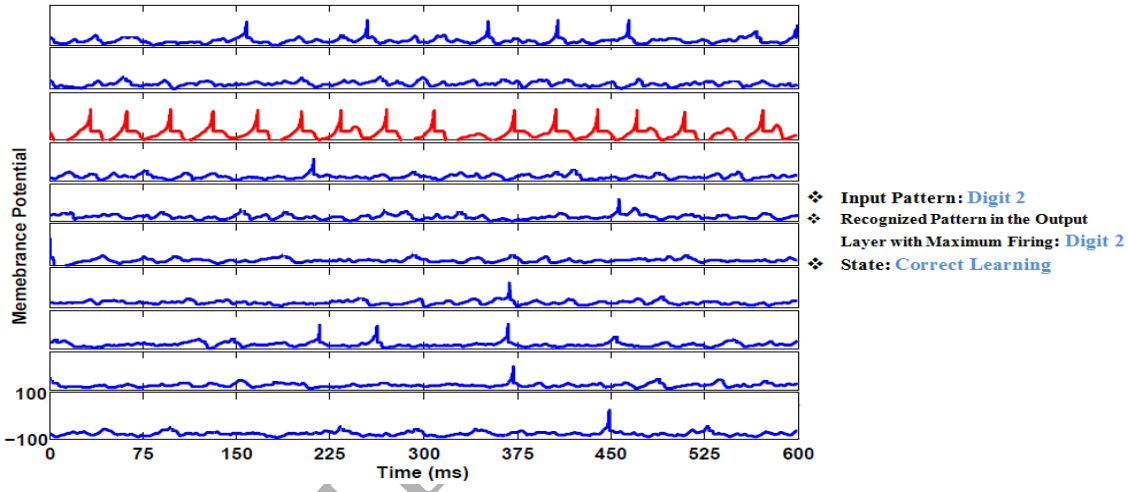
Memebrance Potential
100
−100
0
75
150
225
300
375
450
525
600
Time (ms)
Input Pattern: Digit 2
Recognized Pattern in the Output Layer with Maximum Firing: Digit 2
State: Correct Learning

(c)

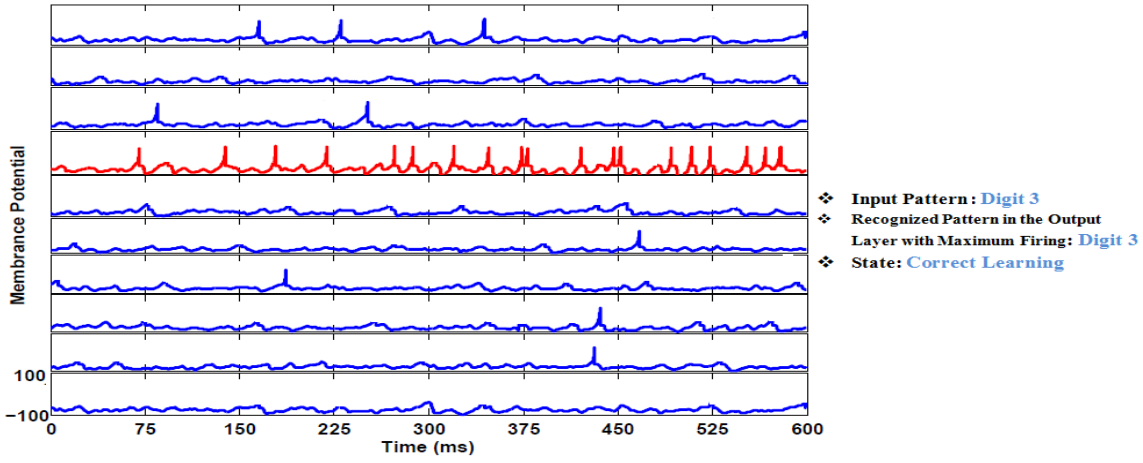
Membrance Potential
100
−100
0
75
150
225
300
375
450
525
600
Time (ms)
Input Pattern: Digit 3
Recognized Pattern in the Output Layer with Maximum Firing: Digit 3
State: Correct Learning

(d)

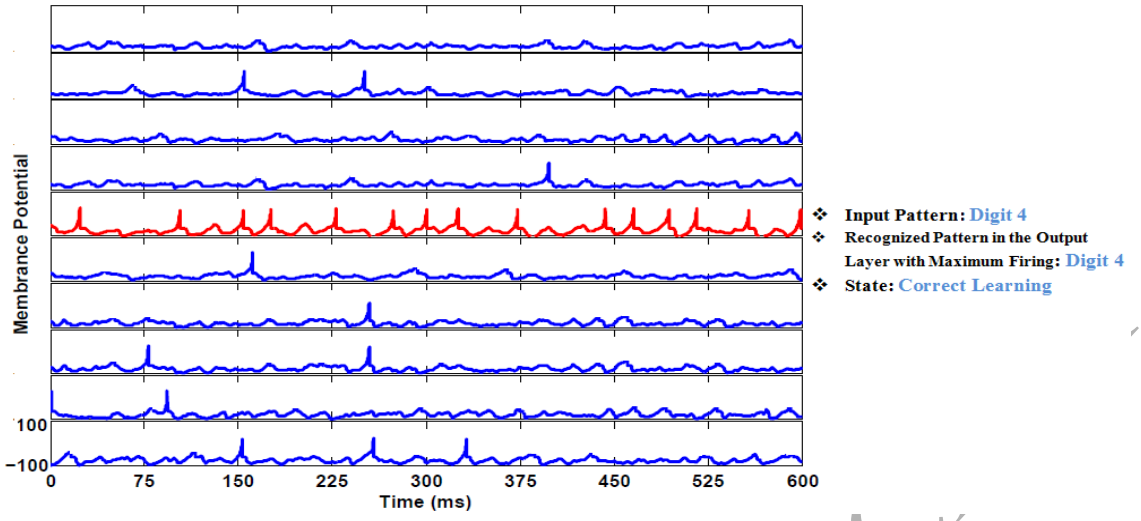

(e)

Fig.10: (a-e) show spike pattern of classifying neurons by presenting digit-tests 0,1,2,3,4 to the input, respectively. The results indicate the performance accuracy of the network.

The results confirm the effectiveness of the proposed learning approach, the rate of correct categorization (96.1%) is better than previous published results. In other words, the proposed learning method based on experimental observations has correct grounds. An interesting point in the results is that the classifying neurons generate sparse spike activity in response to the input test patterns and they have the most firing rate in response to the patterns that have trained for them. Also, the classifying neurons based on the similarity of the input pattern to the patterns that they are representative of them, indicate spike reaction. The performance accuracy is affected by the spike timings. Therefore, the average result of fifteen run repetitions on MNIST test-set has reported. The standard deviation in fifteen run repetitions is small and equal to 1.08%, which indicates the performance stability of the pattern recognition network.

Simulation results show that three different modes have observed in the results:

Correct learning: The classifying neurons fire proportional to the input digits (96.1%)

Some mistakes: The classifying neurons do not correctly detect their corresponding input (3%)

Always firing: The classifying neurons continuously fire regardless of the input pattern (0.9%)

The first mode of the results has shown in Fig.10. Fig.11 (a),(b) show the "some mistakes" and "always firing" mode of results, respectively. Fig.11(a) shows the case that a sample test of digit 4 has applied to the input and classifying neuron 9 instead of classifying neuron 4 indicated the highest firing rate. Subsequently, as shown in Fig. 11(b), digit 7 has applied to the input and the classifying neurons 1,4,7,9 have the maximum rate of firing.

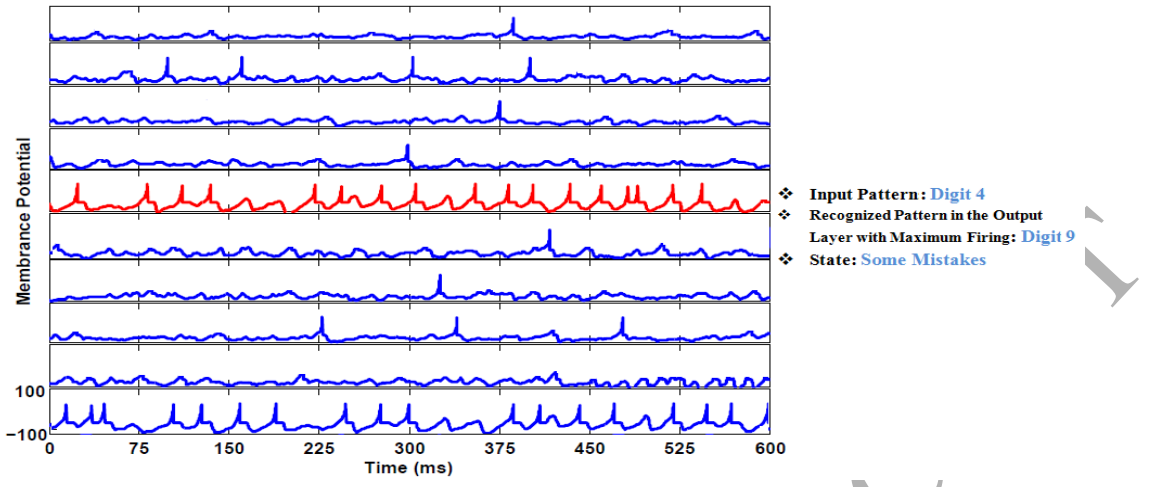

(a)

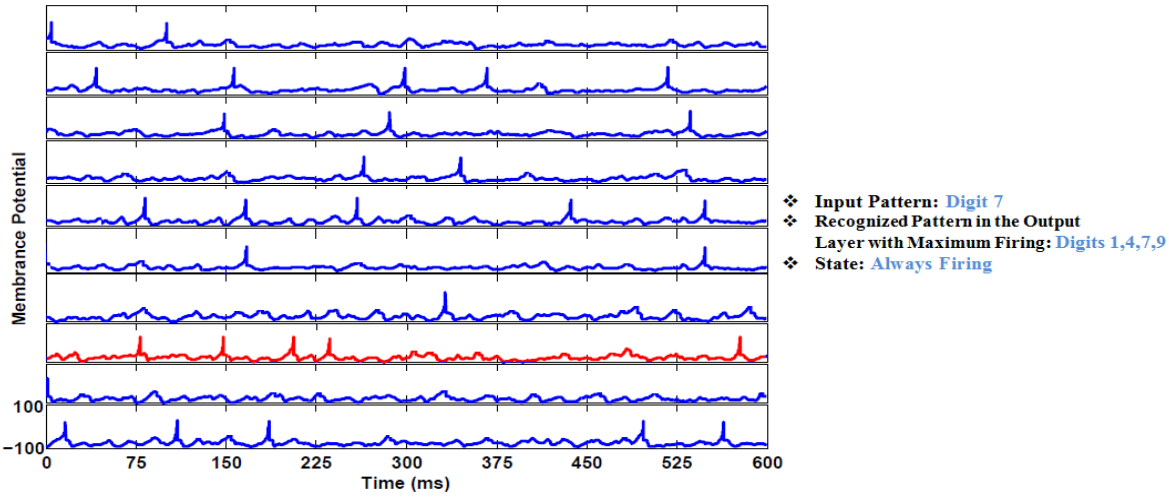

(b)

Fig.11: Performance error when (a) classifying neurons cannot correctly perform the categorization and (b) classifying neurons continuously fire regardless of the input pattern.

According to the training equations (Eqs.8-11), both excitatory synapses (Eqs.8,10) and inhibitory synapses (Eqs.9,11) are trained. The trained synapses reinforce the paths between activated neurons of the second layer and the classifying neurons. Fig.12 presents the evolution of strength of synapses between ten random neurons (#18, #410, #950, #1020, #2400, #3241, #3780, #4000, #4253, #4800) from the second layer and classifying neurons 0,1 during the first training iteration. This evolution shows learning can be seen as the strengths of certain synapses increase to higher levels of initial connectivity value or decrease to the lower level. It should be noted that initial connectivity value of pyramidal neurons and interneurons of second layer to classifying neurons is 0.42 and 0.7, respectively.

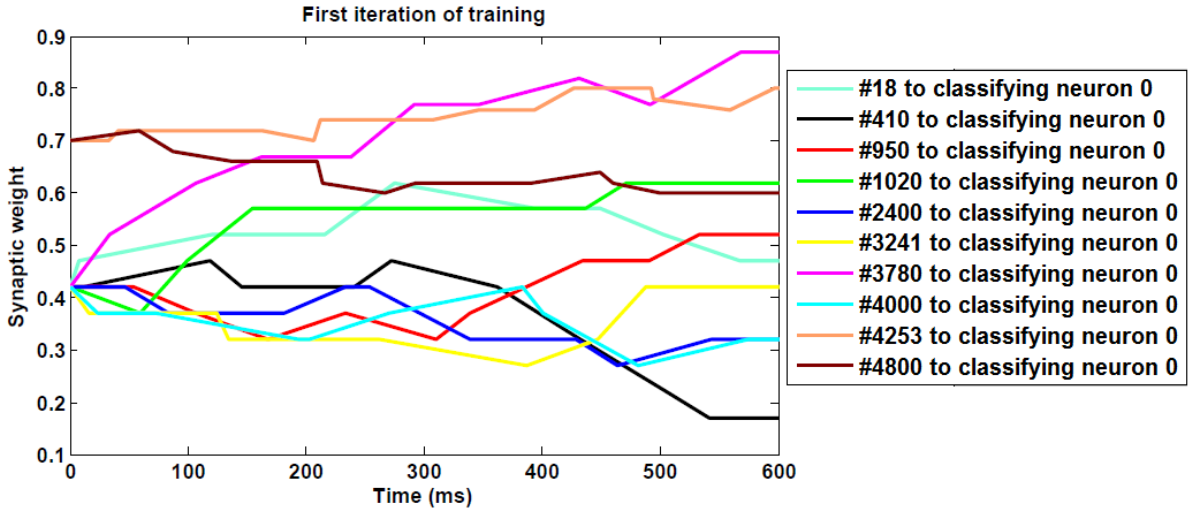

(a)

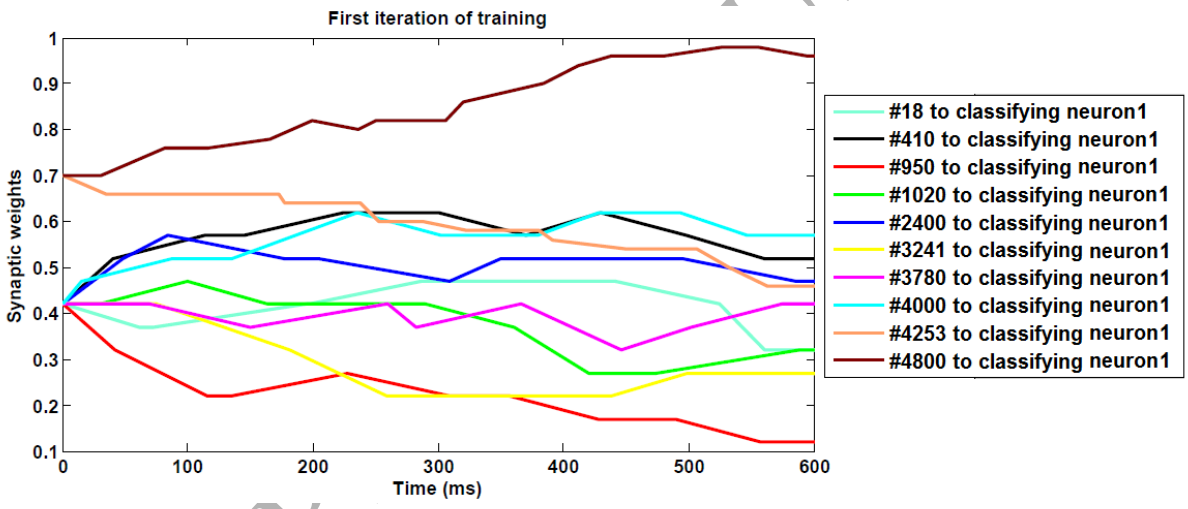

(b)

Fig.12: (a), (b) shows change of synaptic weights of ten random neurons of second layer to classifying neurons 0, 1 during first training iteration.

The second layer consists of a large number of neurons, and it is not possible to show the spike activity of all neurons. On the other hand, spiking activity of the limited number of pyramidal neurons and interneurons can't be considered as the overall behavior of the second layer neurons. Therefore, the number of spikes per neuron in the first iteration of training and the test stage (after training) is shown in Fig.13. All neurons were arranged in the form of a rectangular matrix with 100*50 arrays (4000-PY+1000-IN=5000 neurons), and the number of spike activity during the interval of 600 ms of first

iteration of training and test for each neuron is shown in Fig. 13. As is evident, the activity of second layer neurons before and after training is sparse and the average firing rate after training has decreased which make it suitable for the low-power neuromorphic hardware.

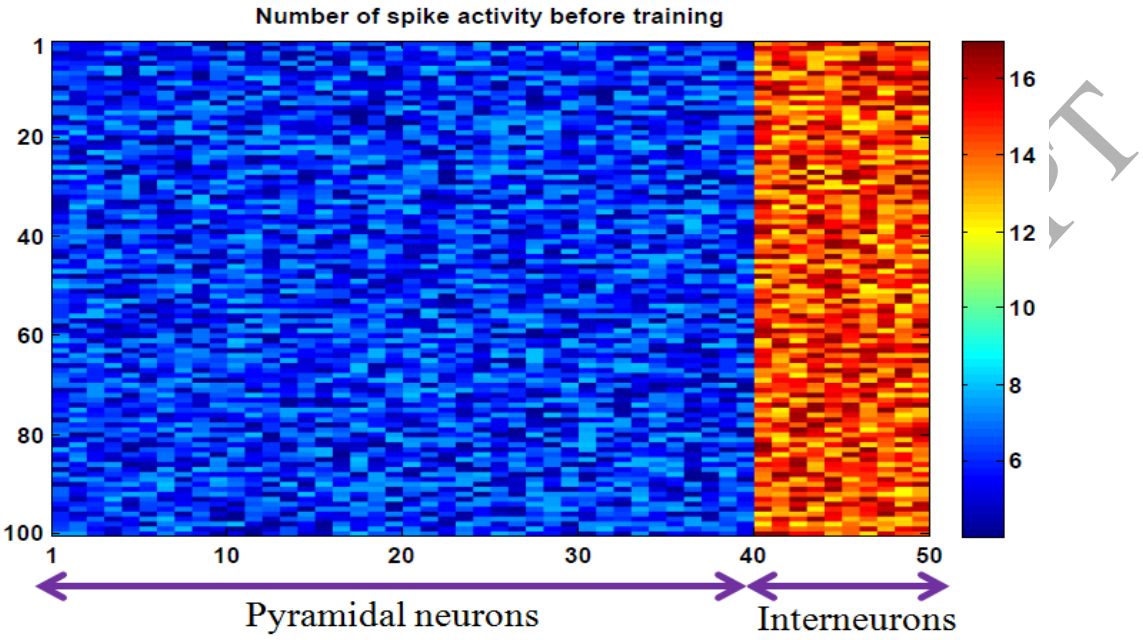

(a)

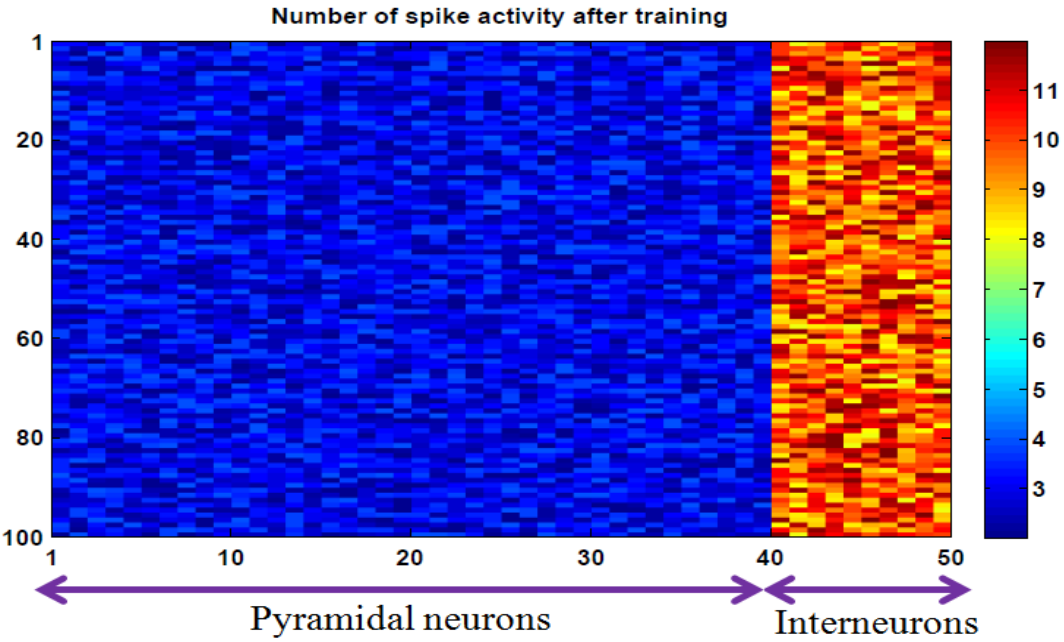

(b)

Fig.13: Number of spike activity of all neurons of second layer, (a) first iteration of training (before training) and (b) first iteration of test (after training). The average firing rate after training has been diminished.

The preciseness of the result in recognizing MNIST patterns with unsupervised exponential STDP effective on AMPA and GABA synaptic currents achieves the best classification performance as high as 96.1%, which the accuracy is higher than previous unsupervised pattern recognition networks. In recent years, some architecture based on spike calculations have introduced in the field of pattern recognition. In Table I, the classification accuracy of the existing spiking architectures on the standard MNIST dataset have summarized. A brief comparison of the present work to the best-published results on MNIST, confirms that proposed bio-inspired pattern recognition network improves the previous state-of-the-art categorization accuracy on MNIST. This article, in turn, confirms that the proposed learning method based on the biological findings of the learning process in brain is an effective way of learning in the machine.

We tried to consider the critical issues in network design. For example, the limitation of the test set and the use of training samples at the stage of testing the network [16,51] restricts the generalization ability of the network; here this point has considered well.

Table. I: Comparison of performance accuracy of the unsupervised pattern recognition networks on MNIST.

Architecture	Preprocessing	Training-type	(Un-)supervised	Learning-rule	#Neurons/ #Synapses	Performance
Two layer network [18]	None	Spike-base	Unsupervised	Rectangular STDP	1184/ 313600	93.5%
Two layer network [24]	None	Spike-base	Unsupervised	Exponential STDP	7184/ 5017600	95%
Proposed network	Image to signal mapping	Spike-base	Unsupervised	Exponential STDP effective on AMPA and GABA synaptic currents	5000/ 5001605	96.1%

Some related works in addition to those reported in the above table have presented in [18, 52-54]. By training the proposed SNN on a portion of the training samples of MNIST, the rate of correct detection decreases (for example recognition accuracy decreases to 95.4% when SNN is trained on 48000 training samples). The highest recognition accuracy of the neural networks on the MNIST dataset has been obtained from training on all 60000 training samples. Also, in some cases, the trained network has been tested on all or part of the testing samples in which we tested our network on all testing samples of

MNIST. The following points outline the distinction and superiority of the proposed pattern recognition network compared to convolutional neural networks.

The recent progress of low-power neuromorphic hardware provides exceptional conditions for applications where their focus is more on saving power. However, the design of spiking neural networks (SNN) to recognize real-world patterns on such hardware remains a major challenge ahead of the researchers. Hardware implementations of spiking neural network that has been done in recent years on the neuromorphic chip [3-6], as a power-efficient system, for transmitting each spike only consume a few nJ or even pJ [7-9]. In some recent cases, consumption is less than 0.02 pJ per spike [10] and consequently only a few pW per synapse [11], so that, the proper performance of neuromorphic systems makes them possible to implement on-chip learning mechanisms on these hardware [4,12-13]. In this paper, SNN inspired by the model of local cortical population proposed based on the mechanisms used in the neuromorphic platforms, which contain exponential synapses with the ability of the STDP learning, excitatory and inhibitory neurons and synapses, and exponential form of STDP learning approach. The distinct difference between convolutional neural network and our bio-inspired pattern recognition network is that we modeled more biologically possible structure [55,27] with the ability to implement on some neuromorphic hardware because of the existence exponential excitatory and inhibitory synapses (AMPA and GABA receptor dynamics), excitatory and inhibitory neurons, and exponential STDP learning mechanism in synapses. The second difference includes the sparse spike-based learning (learning method is based on sparse firing activity of neurons), which this point is essential for the power consumption of neuromorphic hardware when the learning process takes up a considerable part of time. Therefore, in the case that the proposed SNN will be implemented on the low power neuromorphic boards [56-59] such as IBM's TrueNorth chip [59], it will consume about 0.36 mW because the power consumption of this chip is 72 mW per 1 million neurons which is a very low power consumption for the vision processors. The Third difference summarizes in the informative signal of image based on sequences of PSWFs, which in turn reduces the size of the input layer significantly and generalize the spiking pattern recognition network to other realistic sized image sets. The fourth difference is that the presented training mechanism has defined based on biological evidence of the learning mechanism of brain, which is more analogous to the learning approach accessible on some neuromorphic hardware [57, 60-61].

On the other hand, unlike most previous studies, any class label did not use in the learning procedure of the network. Therefore, the SNN trained with the spike-based **unsupervised** weight optimization based on the dynamical behavior of the excitatory (AMPA) and inhibitory (GABA) synapses using Spike Timing Dependent Plasticity (STDP) which the obtained accuracy on the MNIST outperforms previous unsupervised training methods for spiking pattern recognition networks.

In fact, the proposed pattern recognition network is a liquid state machine (LSM). LSM is a computational model based on the computational neuroscience, which offers promising solutions to real-world applications in both software and hardware-based systems [62-63]. In the standard LSM model, the reservoir involves spiking neurons randomly connected to each other by fixed synapses, which is similar to the second layer of the proposed pattern recognition network, with the difference that dynamics of synapses in the present network designed based on biological evidence of learning. The readout neurons of LSM similar to classifying neurons act as an output layer, which can be trained to conduct classification with good accuracy. The LSM input layer is stimulated by the spike train [64]. In the present paper, the image transforms into the informative signal which converter turn this signal to the Poisson spike trains. Therefore, input, the second layer, and output of the proposed pattern recognition network is similar to LSM and benefit high computing ability. It should be noted, the dynamics of the AMPA and GABA receptors in excitatory and inhibitory synapses, as well as the proposed coding on the image, was proposed for the first time in the structure of the pattern recognition networks.

LSM usually was trained on the synaptic weights of the readout neurons, but there are some studies that were trained on the synaptic weights of the reservoir and readout neurons. The best classification accuracy of LSM, which was trained supervised on the MNIST dataset via the updating the synaptic weights of readout neurons was 91.4%. Also, the best classification accuracy of D-LSM (Deep LSM) with STDP-based unsupervised reservoir tuning and spike-based supervised training for the readout neurons on the 1000 test-set of MNIST was 95.6% (the present paper reached 96.1% classification accuracy on the all test-set of MNIST) [65]. Therefore, it is obvious that the proposed pattern recognition network with spike-based unsupervised weight optimization based on the dynamical behavior of the excitatory (AMPA) and inhibitory (GABA) synapses reached the best classification accuracy compared to the best LSM architectures.

It should be noted, the proposed pattern recognition network benefits the sparse spike-based learning, which the learning method is based on sparse firing activity of neurons. Therefore, considering that the change in synaptic weights in STDP-based training method is based on the spike activity of neurons, it is not necessary to train the huge amount of weights within the second layer and the computational cost is not high, which this point is essential for the energy efficient neuromorphic hardware.

Table.II shows the performance accuracy of the proposed spiking pattern recognition platform with respect to the number of neurons in the second layer. It should be emphasized that the structure of the second layer independent of the neuron number has adapted from the local cortical population. Therefore, the second layer structure, the existence probability of the synapse between neurons, the ratio of pyramidal neurons to interneurons is constant. Only the effect of changing the number of neurons on the classification accuracy was examined. Table. II indicates that with increasing neuron number up to 5000,

the accuracy with the ascending trend is changing and in neuron numbers above 5000, there is little change in the accuracy of the network performance. The rate of correct detection validates the effectiveness and efficiency of the proposed pattern recognition network.

Table. II: The performance accuracy of the pattern recognition network versus the number of neurons in the second layer.

Number of neurons In second layer	PY: 2000 IN: 500 All: 2500	PY: 3200 IN: 800 All: 4000	PY: 4000 IN: 1000 All: 5000	PY: 6000 IN: 1500 All: 7500
Performance	86.7%	93.6%	96.1%	96.8%

4- Conclusion

Support vector machine, maximum entropy classifier, Naïve Bayes classifier, decision trees and perceptron are various methods for pattern recognition. These methods have the weak biological aspect. Because of this, spiking neural networks surpassed various previous machine-learning tools due to their good biological backgrounds so that many studies have shown the higher computational power of biologically inspired system adapted from brain structure [66,26]. In this regards, the spiking pattern recognition network based on the computational model of cortical was designed. The present paper attempts to build and train a network of integrate-and-fire neurons with biologically realistic synaptic connection based on the computational model of AMPA and GABA current for excitatory and inhibitory synapses. Past research introduced the STDP as a bio-inspired learning rule in spiking networks that can be used to extract input characteristics by the unsupervised approach. On the other hand, the change in synaptic weights has known as a mechanism for the information storing and memory in the brain based on LTP and LTD; some studies proved that LTP and LTD are the two dominant cell activity models in synaptic plasticity [67-68]. Therefore based on some experimental evidence, the proposed training method has defined on the spike time dependent plasticity, which has affected AMPA-type and GABA-type currents. After the completion of training, the pattern recognition network as a biological neuro-computing resource can identify digits of MNIST test-set with high accuracy 96.1%. Spike activity in the network was sparse, which this feature makes it suitable for fast, energy-efficient neuromorphic hardware platform. One problem in digit recognition with SNN is realistic sized images so that, correspondence one by one image pixels with input layer neurons reduces the computational speed and increase the number of neurons in the input layer. In this paper, we overcome with this problem using the informative signal of image based on sequences of PSWFs. Finally, according to the reported results, proposed learning

algorithm and the image pre-processing in compared to previous related works in digit recognition can operate more accurately.

References

[1] Sengupta, B., Stemmler, M. B., & Friston, K. J. (2013). Information and efficiency in the nervous system—a synthesis. PLoS Comput Biol, 9(7), e1003157.
[2] Nazari, S., Amiri, M., Faez, K., & Amiri, M. (2015). Multiplier-less digital implementation of neuron–astrocyte signalling on FPGA. *Neurocomputing*, *164*, 281-292.
[3] Diaz, C., Sanchez, G., Duchen, G., Nakano, M., & Perez, H. (2016). An efficient hardware implementation of a novel unary spiking neural network multiplier with variable dendritic delays. *Neurocomputing*, *189*, 130-134.
[4] Wang, Q., Li, Y., Shao, B., Dey, S., & Li, P. (2017). Energy efficient parallel neuromorphic architectures with approximate arithmetic on FPGA. *Neurocomputing*, *221*, 146-158.
[5] Haghiri, S., Ahmadi, A., & Saif, M. (2016). VLSI implementable neuron-astrocyte control mechanism. *Neurocomputing*, *214*, 280-296.
[6] Maguire, L. P., McGinnity, T. M., Glackin, B., Ghani, A., Belatreche, A., & Harkin, J. (2007). Challenges for large-scale implementations of spiking neural networks on FPGAs. *Neurocomputing*, *71*(1), 13-29.
[7] Indiveri, G., & Liu, S. C. (2015). Memory and information processing in neuromorphic systems. Proceedings of the IEEE, 103(8), 1379-1397.
[8] Merolla, P., Arthur, J., Akopyan, F., Imam, N., Manohar, R., & Modha, D. S. (2011, September). A digital neurosynaptic core using embedded crossbar memory with 45pJ per spike in 45nm. In Custom Integrated Circuits Conference (CICC) IEEE, (pp. 1-4).
[9] Furber, S. (2016). Large-scale neuromorphic computing systems. Journal of Neural Engineering, 13(5), 051001.
[10] Azghadi, M. R., Iannella, N., Al-Sarawi, S., & Abbott, D. (2014). Tunable low energy, compact and high performance neuromorphic circuit for spike-based synaptic plasticity. PloS one, 9(2), e88326.
[11] Azghadi, M. R., Iannella, N., Al-Sarawi, S. F., Indiveri, G., & Abbott, D. (2014). Spike-based synaptic plasticity in silicon: design, implementation, application, and challenges. Proceedings of the IEEE, 102(5), 717-737.
[12] Qiao, N., Mostafa, H., Corradi, F., Osswald, M., Stefanini, F., Sumislawska, D., & Indiveri, G. (2015). A reconfigurable on-line learning spiking neuromorphic processor comprising 256 neurons and 128K synapses. Frontiers in neuroscience, 9, 141.
[13] Basu, A., Shuo, S., Zhou, H., Lim, M. H., & Huang, G. B. (2013). Silicon spiking neurons for hardware implementation of extreme learning machines. *Neurocomputing*, *102*, 125-134.
[14] Liu, D., & Yue, S. (2017). Fast unsupervised learning for visual pattern recognition using spike timing dependent plasticity. *Neurocomputing*, *249*, 212-224.
[15] Beyeler, M., Dutt, N. D., & Krichmar, J. L. (2013). Categorization and decision-making in a neurobiologically plausible spiking network using a STDP-like learning rule. Neural Networks, 48, 109-124.
[16] Brader, J. M., Senn, W., & Fusi, S. (2007). Learning real-world stimuli in a neural network with spike-driven synaptic dynamics. Neural computation, 19(11), 2881-2912.
[17] Mohemmed, A., Schliebs, S., Matsuda, S., & Kasabov, N. (2013). Training spiking neural networks to associate spatio-temporal input–output spike patterns. *Neurocomputing*, *107*, 3-10.
[18] Querlioz, D., Bichler, O., Dollfus, P., & Gamrat, C. (2013). Immunity to device variations in a spiking neural network with memristive nanodevices. IEEE Transactions on Nanotechnology, 12(3), 288-295.
[19] Lin, Z., Ma, D., Meng, J., & Chen, L. (2017). Relative ordering learning in spiking neural network for pattern recognition. *Neurocomputing*.

[20] Rumelhart, D. E., Hinton, G. E., & Williams, R. J. (1985). Learning internal representations by error propagation (No. ICS-8506). California Univ San Diego La Jolla Inst for Cognitive Science.
[21] Mesnard, T., Gerstner, W., & Brea, J. (2016). Towards deep learning with spiking neurons in energy based models with contrastive Hebbian plasticity. arXiv preprint arXiv:1612.03214.
[22] O'Connor, P., Neil, D., Liu, S. C., Delbruck, T., & Pfeiffer, M. (2013). Real-time classification and sensor fusion with a spiking deep belief network. Frontiers in neuroscience, 7.
[23] Neil, D., & Liu, S. C. (2014). Minitaur, an event-driven FPGA-based spiking network accelerator. IEEE Transactions on Very Large Scale Integration (VLSI) Systems, 22(12), 2621-2628.
[24] Diehl, P. U., & Cook, M. (2015). Unsupervised learning of digit recognition using spike-timing-dependent plasticity. *Frontiers in computational neuroscience*, *9*.
[25] Tissera, M. D., & McDonnell, M. D. (2016). Deep extreme learning machines: supervised autoencoding architecture for classification. *Neurocomputing*, *174*, 42-49.
[26] Zhang, M., Qu, H., Xie, X., & Kurths, J. (2017). Supervised learning in spiking neural networks with noise-threshold. *Neurocomputing*, *219*, 333-349.
[27] Mazzoni, A., Panzeri, S., Logothetis, N. K., & Brunel, N. (2008). Encoding of naturalistic stimuli by local field potential spectra in networks of excitatory and inhibitory neurons. *PLoS Comput Biol*, *4*(12), e1000239.
[28] McCormick, D. A., Connors, B. W., Lighthall, J. W., & Prince, D. A. (1985). Comparative electrophysiology of pyramidal and sparsely spiny stellate neurons of the neocortex. *Journal of neurophysiology*, *54*(4), 782-806.
[29] Meijer, P. B. (1992). An experimental system for auditory image representations. *IEEE transactions on biomedical engineering*, *39*(2), 112-121.
[30] Slepian, D., & Pollak, H. O. (1961). Prolate spheroidal wave functions, Fourier analysis and uncertainty—I. *Bell System Technical Journal*, *40*(1), 43-63.
[31] Nazari, S., & Janahmadi, M. (2018). A new approach to detect the coding rule of the cortical spiking model in the information transmission. Neural Networks, 99, 68-78.
[32] Braitenberg, V., & Schüz, A. (2013). Anatomy of the cortex: statistics and geometry (Vol. 18). Springer Science & Business Media.
[33] Tuckwell, H. C. (2005). Introduction to theoretical neurobiology: volume 2, nonlinear and stochastic theories (Vol. 8). Cambridge University Press.
[34] S. Furber, "Large-scale neuromorphic computing systems," Journal of neural engineering, vol. 13, no. 5, pp. 1-14, 2016.
[35] Nazari, S., Faez, K., Amiri, M., & Karami, E. (2015). A digital implementation of neuron–astrocyte interaction for neuromorphic applications. *Neural Networks*, *66*, 79-90.
[36] Nawrocki, R. A., Voyles, R. M., & Shaheen, S. E. (2016). A mini review of neuromorphic architectures and implementations. *IEEE Transactions on Electron Devices*, *63*(10), 3819-3829.
[37] Ardakani, A., Condo, C., & Gross, W. J. (2016). Sparsely-connected neural networks: towards efficient VLSI implementation of deep neural networks. *arXiv preprint arXiv:1611.01427*.
[38] Sjöström, P. J., Turrigiano, G. G., & Nelson, S. B. (2001). Rate, timing, and cooperativity jointly determine cortical synaptic plasticity. *Neuron*, *32*(6), 1149-1164.
[39] Holmgren, C., Harkany, T., Svennenfors, B., & Zilberter, Y. (2003). Pyramidal cell communication within local networks in layer 2/3 of rat neocortex. *The Journal of physiology*, *551*(1), 139-153.
[40] Izhikevich, E. M. (2004). Which model to use for cortical spiking neurons?. *IEEE transactions on neural networks*, *15*(5), 1063-1070.
[41] Diaz, C., Frias, T., Sanchez, G., Perez, H., Toscano, K., & Duchen, G. (2017). A novel parallel multiplier using spiking neural P systems with dendritic delays. *Neurocomputing*, *239*, 113-121.
[42] Chen, Q., Wang, J., Yang, S., Qin, Y., Deng, B., & Wei, X. (2017). A real-time FPGA implementation of a biologically inspired central pattern generator network. *Neurocomputing*, *244*, 63-80.
[43] Sidaty, N., Larabi, M. C., & Saadane, A. (2017). Toward an audiovisual attention model for multimodal video content. *Neurocomputing*.

[44] Eskandari, E., Ahmadi, A., & Gomar, S. (2016). Effect of spike-timing-dependent plasticity on neural assembly computing. *Neurocomputing*, *191*, 107-116.
[45] Ferrández, J. M., Lorente, V., de la Paz, F., & Fernández, E. (2013). Training biological neural cultures: Towards Hebbian learning. *Neurocomputing*, *114*, 3-8.
[46] Bi, G. Q., & Poo, M. M. (1998). Synaptic modifications in cultured hippocampal neurons: dependence on spike timing, synaptic strength, and postsynaptic cell type. *Journal of neuroscience*, *18*(24), 10464-10472.
[47] Shepherd, J. D., & Huganir, R. L. (2007). The cell biology of synaptic plasticity: AMPA receptor trafficking. *Annu. Rev. Cell Dev. Biol.*, *23*, 613-643.
[48] Shepherd, J. D., & Huganir, R. L. (2007). The cell biology of synaptic plasticity: AMPA receptor trafficking. *Annu. Rev. Cell Dev. Biol.*, *23*, 613-643.
[49] Darian-Smith, C., & Gilbert, C. D. (1994). Axonal sprouting accompanies functional reorganization in adult cat striate cortex. Nature, 368(6473), 737-740.
[50] Skangiel-Kramska, J., Głażewski, S., Jabłońska, B., Siucińska, E., & Kossut, M. (1994). Reduction of GABA A receptor binding of [3 H] muscimol in the barrel field of mice after peripheral denervation: transient and long-lasting effects. Experimental brain research, 100(1), 39-46.
[51] Neftci, E., Das, S., Pedroni, B., Kreutz-Delgado, K., & Cauwenberghs, G. (2013). Event-driven contrastive divergence for spiking neuromorphic systems.
[52] Murru, N., & Rossini, R. (2016). A Bayesian approach for initialization of weights in backpropagation neural net with application to character recognition. *Neurocomputing*, *193*, 92-105.
[53] Qu, B. Y., Lang, B. F., Liang, J. J., Qin, A. K., & Crisalle, O. D. (2016). Two-hidden-layer extreme learning machine for regression and classification. *Neurocomputing*, *175*, 826-834.
[54] Peng, Y., Zheng, W. L., & Lu, B. L. (2016). An unsupervised discriminative extreme learning machine and its applications to data clustering. *Neurocomputing*, *174*, 250-264.
[55] Abbott, L. F., & Song, S. (1999). Temporally Asymmetric Hebbian Learning, Spike liming and Neural Response Variability. In Advances in neural information processing systems (pp. 69-75).
[56] Benjamin, B. V., Gao, P., McQuinn, E., Choudhary, S., Chandrasekaran, A. R., Bussat, J. M., ... & Boahen, K. (2014). Neurogrid: A mixed-analog-digital multichip system for large-scale neural simulations. Proceedings of the IEEE, 102(5), 699-716.
[57] Indiveri, G., Chicca, E., & Douglas, R. J. (2006). A VLSI array of low-power spiking neurons and bistable synapses with spike-timing dependent plasticity. IEEE transactions on neural networks, 17(1).
[58] Khan, M. M., Lester, D. R., Plana, L. A., Rast, A., Jin, X., Painkras, E., & Furber, S. B. (2008, June). SpiNNaker: mapping neural networks onto a massively-parallel chip multiprocessor. In Neural Networks, 2008. IJCNN 2008.(IEEE World Congress on Computational Intelligence). IEEE International Joint Conference on (pp. 2849-2856). Ieee.
[59] Merolla, P. A., Arthur, J. V., Alvarez-Icaza, R., Cassidy, A. S., Sawada, J., Akopyan, F., ... & Brezzo, B. (2014). A million spiking-neuron integrated circuit with a scalable communication network and interface. Science, 345(6197), 668-673.
[60] Diehl, P. U., & Cook, M. (2014, January). Efficient implementation of STDP rules on SpiNNaker neuromorphic hardware. In IJCNN (pp. 4288-4295).
[61] Galluppi, F., Lagorce, X., Stromatias, E., Pfeiffer, M., Plana, L. A., Furber, S. B., & Benosman, R. B. (2015). A framework for plasticity implementation on the SpiNNaker neural architecture. Frontiers in neuroscience, 8, 429.
[62] Natschläger, T., Maass, W., & Markram, H. (2002). The" liquid computer": A novel strategy for real-time computing on time series. *Special issue on Foundations of Information Processing of TELEMATIK*, *8*(LNMC-ARTICLE-2002-005), 39-43.
[63] Li, X., Chen, Q., & Xue, F. (2017). Biological modelling of a computational spiking neural network with neuronal avalanches. *Phil. Trans. R. Soc. A*, *375*(2096), 20160286.
[64] Zhang, Y., Li, P., Jin, Y., & Choe, Y. (2015). A digital liquid state machine with biologically inspired learning and its application to speech recognition. *IEEE transactions on neural networks and learning systems*, *26*(11), 2635-2649.

[65] Wang, Q., & Li, P. (2016, December). D-LSM: Deep Liquid State Machine with unsupervised recurrent reservoir tuning. In *Pattern Recognition (ICPR), 2016 23rd International Conference on* (pp. 2652-2657). IEEE.
[66] Xie, X., Qu, H., Yi, Z., & Kurths, J. (2017). Efficient training of supervised spiking neural network via accurate synaptic-efficiency adjustment method. *IEEE transactions on neural networks and learning systems*, *28*(6), 1411-1424.
[67] Martin, S. J., Grimwood, P. D., & Morris, R. G. (2000). Synaptic plasticity and memory: an evaluation of the hypothesis. Annual review of neuroscience, 23(1), 649-711.
[68] Malenka, R. C., & Bear, M. F. (2004). LTP and LTD: an embarrassment of riches. Neuron, 44(1), 5-21.

Soheila Nazari received the B.Sc. and M.Sc. degrees in electronic engineering from Razi University, Kermanshah, Iran, and the Amirkabir University of Technology, Tehran, Iran, in 2012 and 2014, respectively. She is currently Ph.D. student at Amirkabir University of Technology. Her current research interests include digital circuit design, signal processing, Image Processing, neuromorphic engineering, information theory.

Karim Faez Was born in Semnan, Iran. He received his BSc. degree in Electrical Engineering from Tehran Polytechnic University as the first rank in June 1973, and his MSc. and Ph.D. degrees in Computer Science from University of California at Los Angeles (UCLA) in 1977 and 1980 respectively.

Professor Faez was with Iran Telecommunication Research Center (1981-1983) before Joining Amirkabir University of Technology (Tehran Polytechnic) in Iran in March 1983, where he holds the rank of Professor in the Electrical Engineering Department.

He was the founder of the Computer Engineering Department of Amirkabir University in 1989 and he has served as the first chairman during April 1989-Sept. 1992.

Professor Faez was the chairman of planning committee for Computer Engineering and Computer Science of Ministry of Science, Research and Technology (during 1988-1996).

His research interests are in Biometrics Recognition and authentication, Pattern Recognition, Image Processing, Neural Networks, Signal Processing, Farsi Handwritten Processing, Earthquake Signal Processing, Fault Tolerance System Design, Computer Networks, and Hardware Design.

Dr. Faez coauthored a book in Logic Circuits published by Amirkabir University Press.

He also coauthored a chapter in the book: *Recent Advances in Simulated Evolution and Learning*, Advances in Natural Computation, Vol. 2, Aug.2004,World Scientific.

He published about 300 articles in the above area. He is a member of IEEE, IEICE, and ACM, a member of Editorial Committee of Journal of Iranian Association of Electrical and Electronics Engineers, and International Journal of Communication Engineering.

Emails: kfaez@aut.ac.ir, kfaez@ieee.org, kfaez@m.ieice.org.